CURRENT FRONT STIFFNESS OF EUROPEAN VEHICLES WITH REGARD TO COMPATIBILITY

Jos Huibers
Eric de Beer
TNO Automotive Crash Safety Centre
The Netherlands
Paper No. ID#239

ABSTRACT

EuroNCAP tests are carried out since 1997. The test procedure in general is comparible to the EC Directive 96/79 with a test speed of 64 km/h. This increased test speed implies a higher frontal stiffness for new vehicle designs in order to achieve a high ranking. This frontal stiffness is one of the major factors for compatibility in car to car collisions.

To support the European 4th framework compatibility research activity, load cell barriers are used in ENCAP tests carried out at the TNO Crash Safety Centre and TRL.

In this paper global force displacement characteristics of a number of different vehicle classes are compared and analysed. It will be made clear that small vehicles in the past known not to be strong can produce comparable force levels as large cars. For compatibility this means that in small car against large car collisions the small car's passenger compartment can stay stable and can offer better protection to the occupants, since from accident analyses it is known that serious injury often is caused by high intrusion into the passenger compartment.

For frontal impacts this means that ENCAP tests have driven small cars to increased compatibility for one aspect of compatibility (cabin integrety) at higher speed.

MPV's with high masses and little crushable space show more aggressive force displacement characteristics. This car category is expected to behave less compatible hitting small cars or medium size passenger cars. A longer crushable space for this category is desired, which is in conflict with the special look for these vehicles.

This trend in stiffer vehicle fronts might result in future modifications of the European side impact barrier, which is currently based on average vehicle fronts of old vehicles. This item is only mentioned and will not be further discussed.

INTRODUCTION

Compatibility is an important subject in road traffic safety research, because in a large part of the accidents more than one road user is involved. In that case the passive safety of the different road users is often not very well balanced. This leads to an incompatible situation in which one of the parties suffers from the aggressiveness of the other. During the last two decades, extensive research was done on the statistics of car-to-car crashes giving a/o. interesting rates of aggressiveness, [1,2,3,4,]. Examples of incompatible situations are: a collision of a small and a large car, a collision between a truck and a car or the collision of a car with a pedestrian or cyclist. Nowadays, car-to-car compatibility is an important safety issue for the car industry [5,9] and governmental bodies [2,4,6]. During the last two decades the occupant safety in single car crashes has improved considerably. However, car-to-car crashes still form an increasingly important class of accidents that are examined, [1].

The mass ratio between colliding vehicles (ΔV's for each car involved) is a well known important factor for compatibility, but cannot be influenced. Of course ΔV play's an important role in the average deceleration, but not only ΔV. When ignoring the mass ratio, incompatible crash behaviour further depends on the two other major factors for compatibility, global stiffness (deceleration) and geometrical effects (interaction) [7]. The global stiffness is partly indirect dependent on how the

energy absorbing structure interacts. Good interaction is essential to effectively use the build in global stiffness in order to absorb the impact energy in an early stage of the collision and to avoid intrusion into the passenger cell.

Geometrical incompatibility is strongly related to intrusions of structural car parts into the passenger cabin, which should be avoided as much as possible, since accident investigations have learned that most of serious and fatal injuries are intrusion related. In [8] it is shown that it is very difficult to tackle the question whether or not cars are compatible with respect to these geometrical effects.

An important measure to avoid intrusions is the

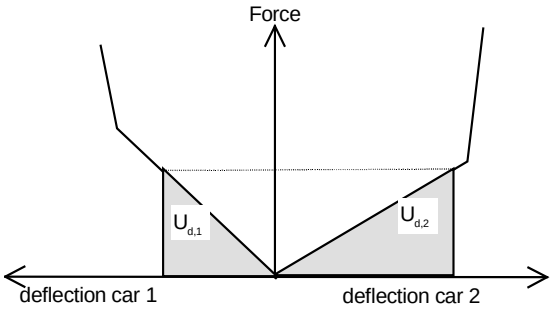

Figure 1 Force balance for small (car1) and large car (car2). Gray area:absorbed energy

design of a frontal crush zone that dissipates as much deformation energy as possible in the case of an accident before the passenger compartment is damaged, e.g. [9]. A way to achieve this is shown in Figure 1. The force deflection curves for the two vehicles allow sufficient energy absorption in both vehicles and increase at certain deformations designed for these particular vehicles in order to be able to take an overload force to avoid intrusion. The structures of both vehicles have to provide good interaction in order to let the forces build up in the designated manner. This means that it should be avoided, for example, that the longitudinals of two colliding cars penetrate each other without deformation of the whole front (the fork-effect) and that the front part of vehicles coincide, which obviously is not the case with cars running into (under) trucks and with collisions between cars and SUV's.

This paper deals with current global vehicle front end stiffnesses like in Figure 1 derived from EuroNcap tests on different car classes.

LOADCELL DATA INFORMATION.

In order to obtain this global stiffness', load cell barriers have been used behind the deformable barrier in the EuroNCAP tests carried out at the TNO Crash Safety Centre and TRL. The objective was to get information about the load distribution and the global stiffnesses (force deflection characteristics) of the vehicle fronts. As there is no clear information available about the barrier intrusion in time, we have to limit ourselves to force displacement characteristics for the vehicle.

The loadcell pattern as used at TRL is displayed in Figure 2.The loadcell pattern and positioning as used at the TNO Crash laboratory is displayed in Figure 3. The measured signals are filtered with CFC60 according to SAEJ211.

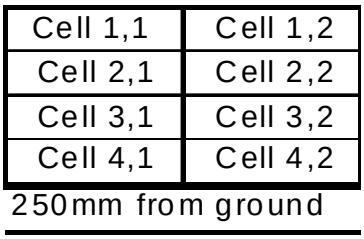

Figure 2 Loadcell arrangement TRL.

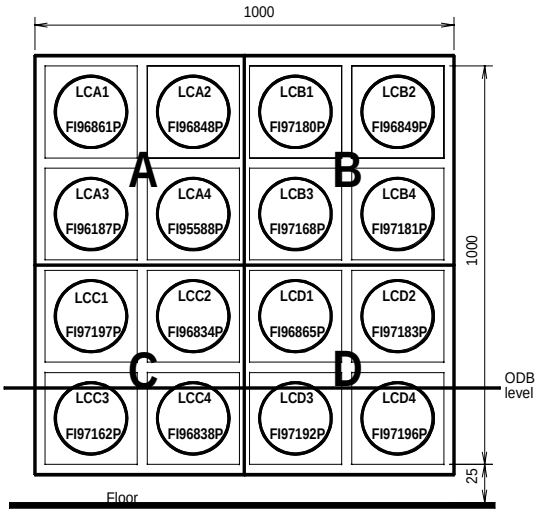

Figure 3 Loadcell arrangement TNO.

The number of cells and pattern differs between the two laboratories. However in the evaluation of the data there is no difference any more, since the level of detail of the TNO data is restricted to left and right half of the load cells (A,C/B,D). Furthermore, most of the TRL tests were carried out with RHD vehicles whereas TNO tests were carried out with LHD cars. For clarification Aup in the figures coincides with Cell 1,1 for TRL loadcell pattern etc.

DATA ANALYSIS

Method

Loadcell data was not collected in the first series of ENCAP tests. For the tests with missing loadcell data, the global force displacement characteristics were obtained by multiplying the measured acceleration with the test mass of the vehicle (m*a). For the acceleration the B pillar base signal of the impacted side was used filtered with CFC15 (cut off frequency 25kHz according to SAEJ211. The displacement was obtained by double integration of that signal (for all used displacements in this paper). Force displacement (FD) characteristics obtained in this way are an approximation because during the crash the active mass reduces. This reduction is partly compensated by the mass of the occupants, coming into effect later in the crash. To get an impression of this approximation FD curves obtained from the loadcell data were compared with FD curves from the m*a approximation. This is done for each car analysed. When looking to the majority of approximations it could be concluded that the m*a curves correlated well with the loadcell curves, with some exceptions.

In some occasions like the Audi A6, it was likely that the differences were caused by the engine contact with the barrier, like sliding off the edge of the barrier later in the crash event.

Car Categories

The cars, which were analysed, were put as much as possible in the same categories as used in the ENCAP phases. Some cars of category phase 3 were tested later as the official phase 3 release but were put in this category because of the size. The cars, which have been analysed, are summarised in Table 1.

Data was analysed of phases 3, the medium size family cars, phase 4 the large saloon/executive cars, phase 6 MPV's and phase 7a/7b small family cars.

Table 1

Sample of the analysed cars.

CAR CATEGORY	KERB MASS KG	TEST MASS KG	SPEED M/S
Phase 3 medium size family cars			
Volkswagen Golf	1140	1336	17.8
Citroen Xsara	1080	1100	17.8
Mitsubishi Lancer	1244	1257	17.8
Renault Megane	1060	1296	17.8
Suzuki Baleno	960	1170	17.8
Toyota Corolla	1060	1275	17.8
VW Beatle	1228	1518	17.8
Ford Focus	1080	1383	17.9
Opel Astra	1100	1325	17.8
Ford Escort	1080	1363	17.9
Mercedes A	1070	1267	17.8
Phase 4 large saloon cars			
BMW 520I	1485	1682	17.9
Saab 95	1485	1713	17.7
Toyota Camry	1385	1604	17.8
Mercedes E200	1440	1650	17.8
Opel Omega	1455	1666	17.8
Audi A6	1400	1663	17.8
Volvo S70	1430	1597	17.8
Phase 6 MPV's			
Renault Espace	1520	1713	17.9
Chrysler Voyager	1800	2040	17.8
Mitsubishi. Space Wagon	1570	1768	17.9
VW Sharan	1690	1906	18.0
Peugeot 806	1550	1748	17.8
Vauxhall Sintra	1650	1933	17.8
Phase 7 small family cars			
Lancia Ypsilon 7a	895	1136	17.8
Renault Clio	xxx	1150	17.8
VW Polo	xxx	1174	17.8
Seat Ibiza	xxx	1227	17.9
Peugeot 206	xxx	1193	17.8
Citroen Saxo	xxx	1051	17.8

For all the cars the following output was generated.

- Force time history for load cell data. In case of TNO data the level of detail was reduced to two columns horizontally and 4 rows vertically, which is similar to the TRL data. Each upper and lower segment part were added up to get the total for the segment and all segments were added up to get the total barrier force.
- Force displacement/m*a for the total barrier force.
- Force displacement summary of each category + average force displacement of each category where this average was obtained by averaging both displacements and forces for the same data points.

Not all the analysed data will be discussed and presented here for each car. However the summary figures of the force displacement data for all the cars will be discussed.

Phase 3 medium size family car analysis.

Figure 4 shows the force displacement curve for the Ford Focus as an example car of this phase. The figure shows both the curves obtained from the loadcell data and from the multiplication of mass times acceleration. The correlation between loadcell data and m*a (CFC15) looks excellent for this car.

The general observation is that for the first 0.4 m the load keeps about constant over 100 kN. This appears to be the barrier characteristic. After this 0.4 m the force is increasing along an almost linear slope.

Figure 7 shows the force time history of the Ford Focus. The load distribution shows a dominant influence of the engine contact area with the barrier (segment Dup). The position of the side member could not be identified by means of the load distribution. This means that the barrier is a too strong filter for this data. This means also that a more detailed pattern for the load cells does not give more information when using this barrier.

The next car discussed is the Mercedes A class.

Figure 5 Shows the barrier segment loads of the Merceds A. The engine influence is clear (segment Tot D).

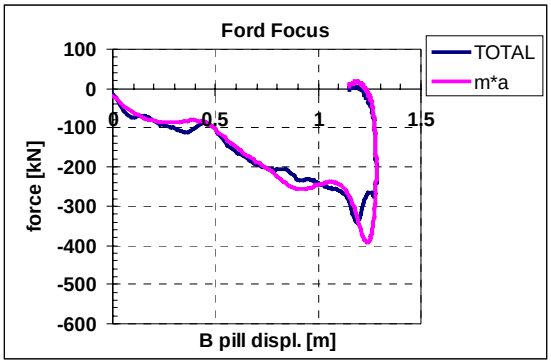

Figure 4 Force Displacement curev Ford Focus

Figure 6 shows the force displacement characteristic. Again a good correlation between loadcell data and m*a (CFC15). Interesting is the steep load increase after 0.4 m displacement even much higher then the Ford Focus , which has a higher mass Table 1. This car is an example of a short crushable space, but able to withstand high loads.

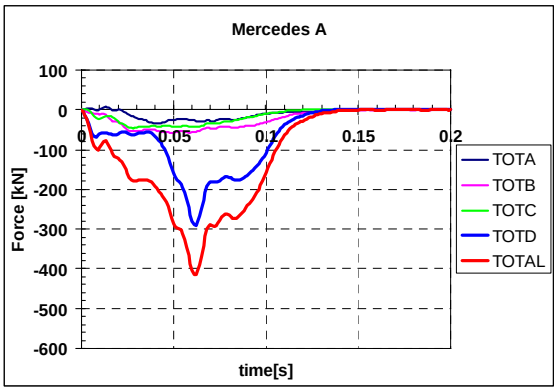

Figure 5 Barrier segment loads Mercedes A

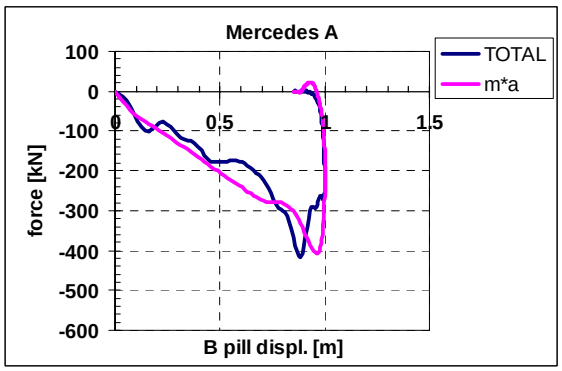

Figure 6 Force Displacement curve Mercedes A

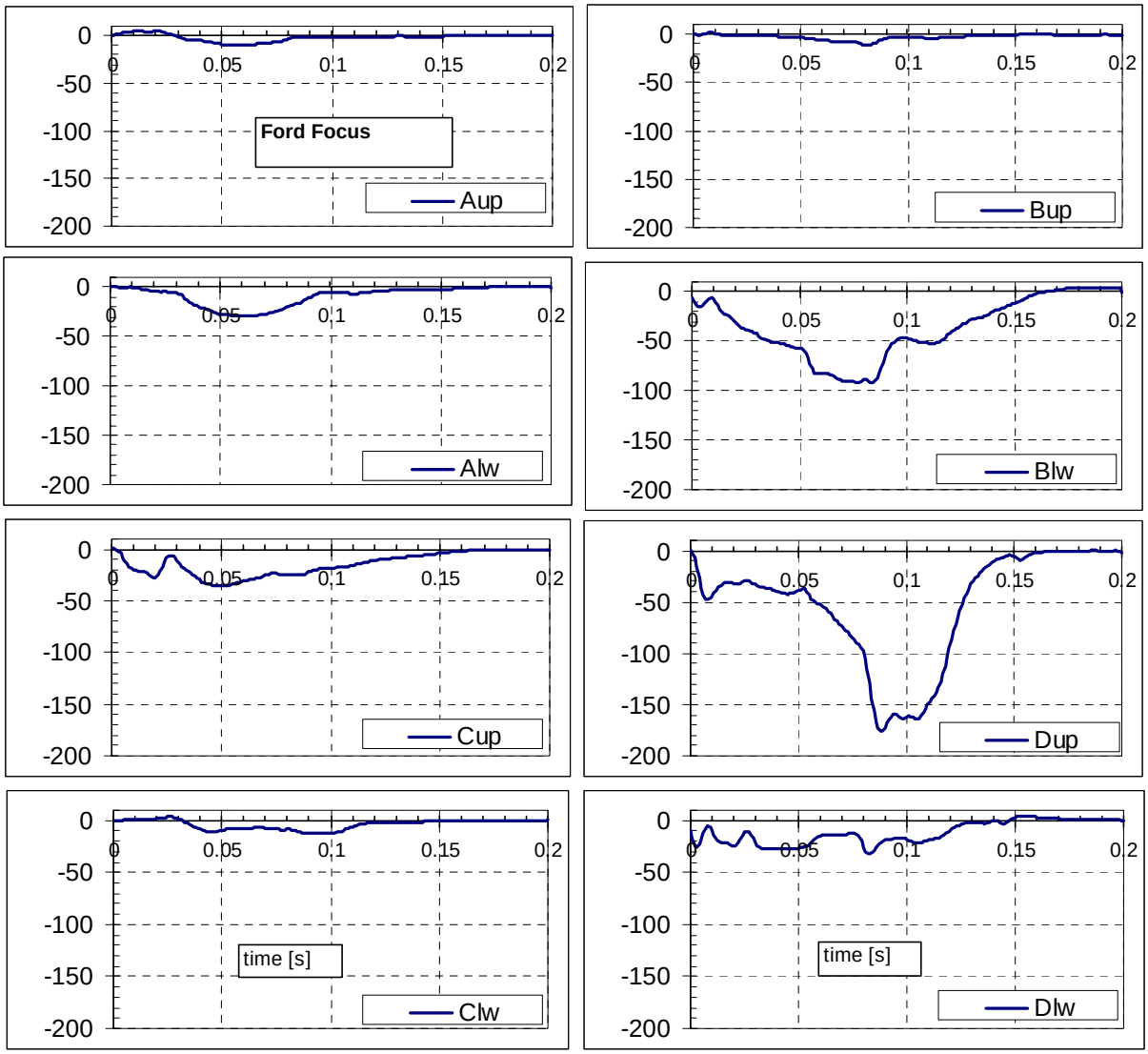

Figure 7 Barrier force pattern [kN] in time Ford Focus

Figure 8 shows the summary and average curve for this phase. Lots of those curves are obtained by means of m*a, as no loadcell data was yet available at this phase. For obtaining this average the Mercedes A class, Ford Escort and VW Beetle were excluded, because of the extreme different behaviour. The Mercedes because of the nature of the concept (short crushable space for this category). The Beetle behaves different to the VW Golf, although based on the same body concept, possibly because of different packaging. The Ford Escort is based on an older concept and shows passenger cell collapse. The Ford focus appeared to be a good representative of the average.

Phase 4 large saloon car analysis

Again loadcell barriers were used for only a few cars. The first car to be discussed is the Mercedes E 200. Figure 9 shows the sum of the barrier segment forces and the total in time. The segment D is the segment where the engine hits and is clearly the dominant segment, like in phase 3. Figure 10 shows the force displacement curve. A good correlation between loadcell data and m*a (CFC15) can be observed.

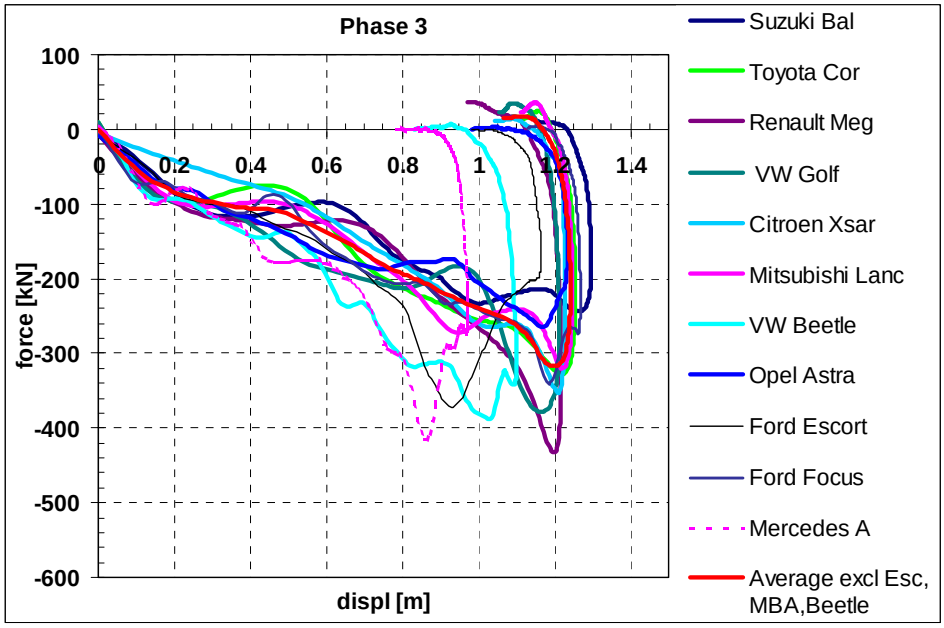

Figure 8 Average force displacments phase 3.

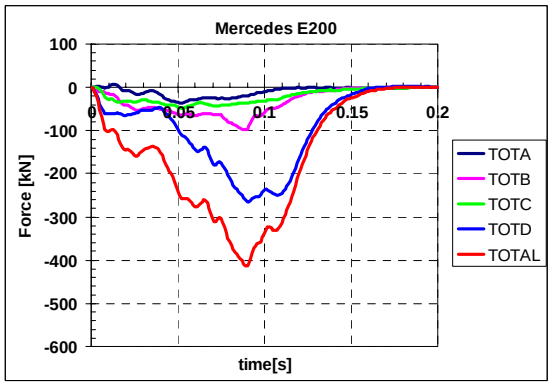

Figure 9 Barrier segment forces Mercedes E 200.

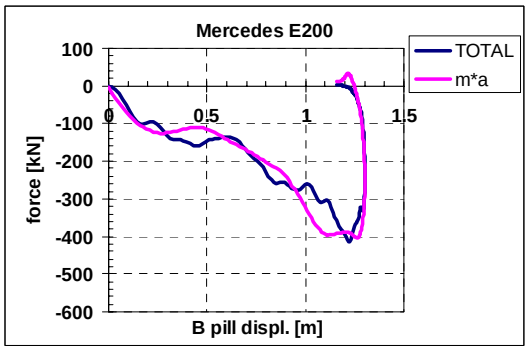

Figure 10 Force displacement curve Mercedes E 200

The next car to be discussed for this phase is the Audi A6.

Figure 11 Shows the barrier segment forces for this car. The shape of the segment-D loads is quite different from the Mercedes E200. The peak is much earlier. This could be caused by early contact of rigid parts of the engine with the rigid barrier.

Figure 12 Shows the force displacement curve. For this car the correlation between loadcell data and m*a (CFC15) is not good. The m*a shows a much more logic shape than the loadcell. The early peak is also visible here. Because of the drop in load before maximum displacement, it looks like the car structure collapses. This could not be concluded from the visual inspection of the car. A possible explanation could be that the engine slides off the rigid barrier edge. Like for phase 3, the area, which is covered by the engine, shows the major contribution to the forces. This is true for all the analysed cars (not shown in this paper).

Figure 13 shows the overview of the force displacement curves for this phase. Most of the curves are obtained by m*a because of the lack of loadcell data.

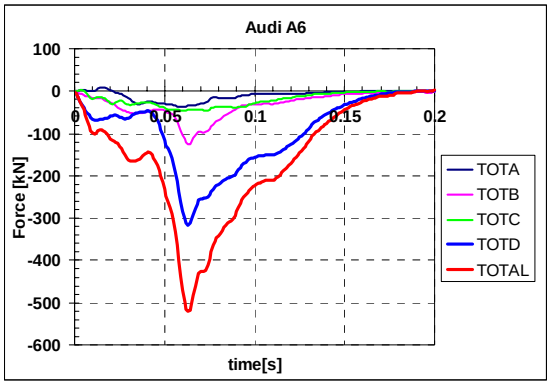

Figure 11 Barrier load cell segments forces Audi A6.

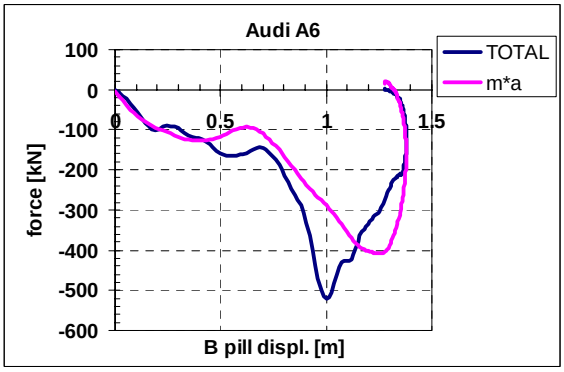

Figure 12 Force diplacement Audi A 6.

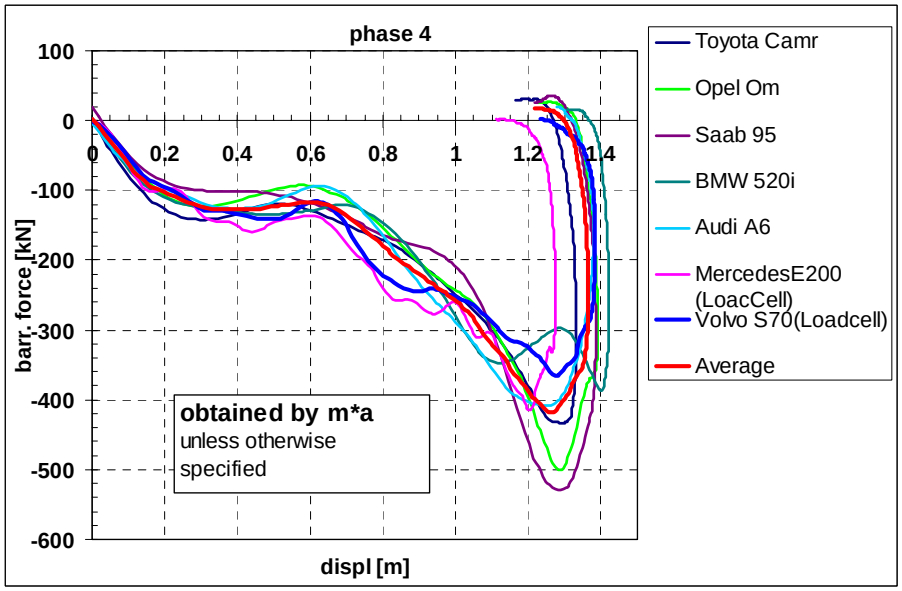

Figure 13 Overview averages phase 4 large saloon cars

Phase 6 MPV analysis

The first car to be discussed is the Renault Espace.

Figure 14 shows the barrier segment loads.

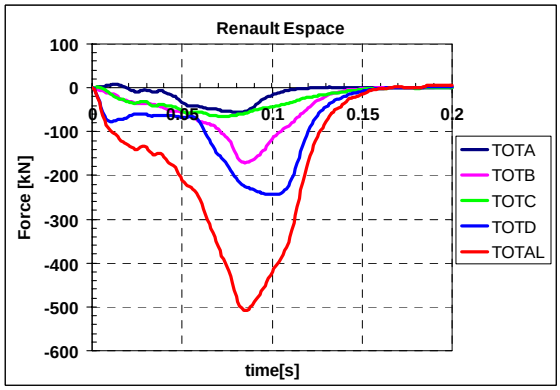

Figure 14 Barrier load cell segments Renault Espace.

Figure 15 shows the force displacements. A good correlation between loadcell data and calculated m*a (CFC15) curves could be observed. The car shows a good stable behavior.

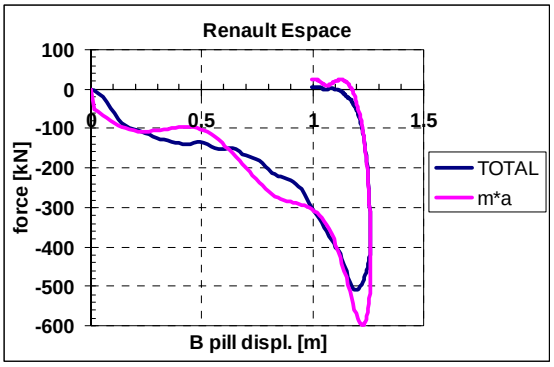

Figure 15 Force displacement Renault Espace.

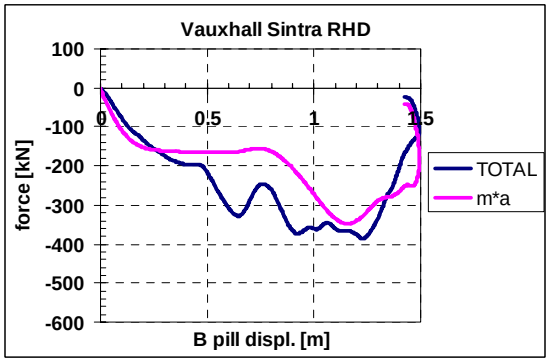

Figure 18 Force displacement Vauxhall Sintra.

The next car shown here is the Vauxhall Sintra.

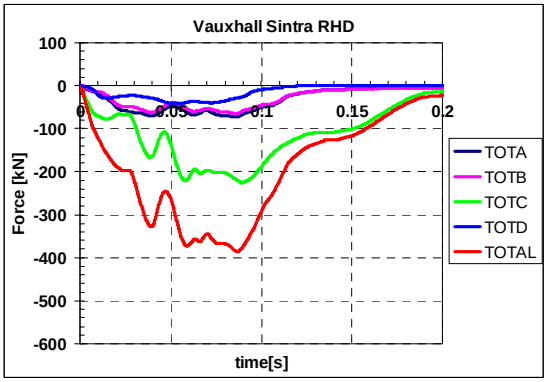

Figure 16 Barrier segment loads Vauxhall Sintra

Figure 16 shows the barrier segment loads for the Vauxhall Sintra. The total load is much lower then the load for the Renault.

Figure 18 shows the force displacement for this car. Looking to the shape it seems that a cabin collapse occurs. Visual inspection of the photographs of the post test confirms this [10]. The correlation between loadcell data and m*a (CFC15) is not good in this case.

Figure 17 shows the overall overview for phase 6 with the average. The average looks a little too low, which is caused by the relative weak Sintra and the Chrysler Voyager, which also shows a cabin collapse later in the crash.

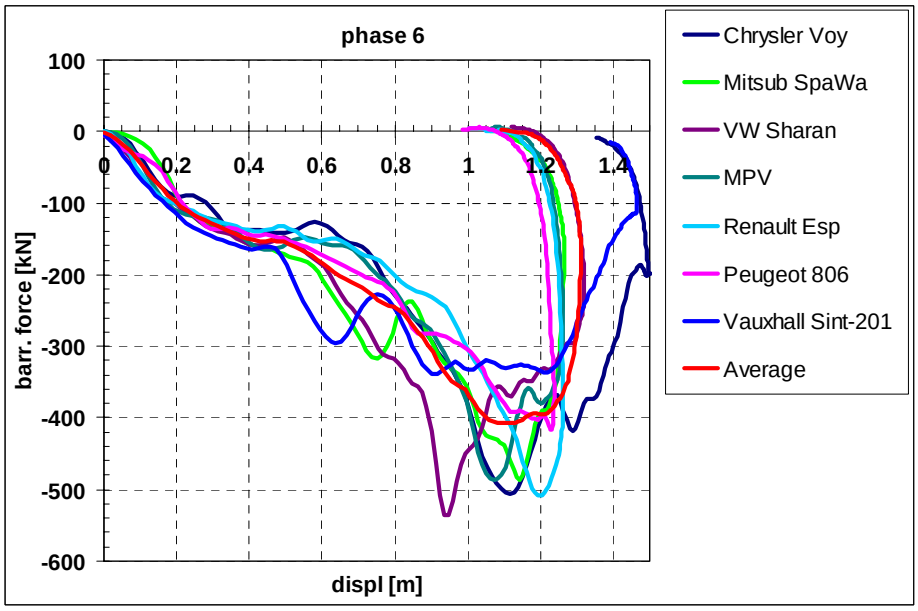

Figure 17 Overview average force diplacements phase 6 MPV's.

Phase 7 small family cars analysis.

Almost all good performers with respect to structural behavior in this phase showed about the same force displacement curves. Only one (good) example will be discussed in detail here, the Renault Clio.

Figure 19 gives the barrier segment loads for the Renault Clio. Good correlation between loadcell data and m*a could be observed.

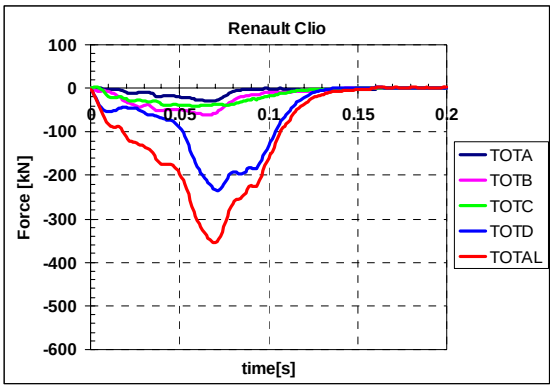

Figure 19 Barrier segment loads Renault Clio.

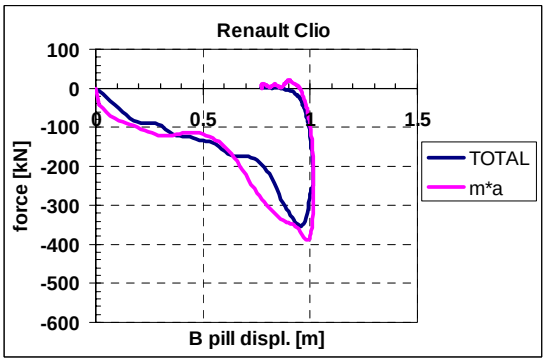

Figure 20 Force displacement Renault Clio

Figure 20 shows the force displacement with excellent correlation between loadcell data and m*a (CFC15).

Figure 21 shows the overview and average of phase 7 cars. Please notice that not all phase 7 cars are represented in this sample. In defining the average the Citroen Saxo was ignored since according to the mass of the vehicle (not considerable different from other cars of this phase) the area under the curve seems to be too small compared with most of the other curves.

Comparison all categories.

Figure 22 shows the average curves for the force displacements for all available phases as discussed here.

Up to 600 mm displacement all the curves look similar ap[art from the MPV's, which show higher forces. At this displacement the MPV's start to progressively increase the loadlevels. For the small family car this rapid increase starts at 800 mm displacement and for the executive cars at about 1150 mm. Up to 1150 mm the curves for the executive and family car coincide very well. The displacement of most of the family cars comes to an end at 1200 mm without a clear increase of the loadlevel. Looking closer to the details of phase 3 results, this increase however was visible for the VW Golf, Renault Megane and Citroen Xsara, but was filtered out by drawing the average curve. This filtering also might be misleading for determining the peak loads. However only m*a data was available for these cars so a good comparison could not be made for these cars compared to cars where loadcell data was available. Some cars (Ford Escort, Ford Focus) show slight higher peak loads.

The masses of the large executive cars don't differ much from the masses of the MPV's, but the general trend is that the displacements of the executive cars are bigger then those of the MPV's. This less available crushable space often results in higher loadlevels for the MPV's at lower deformation. Only two out of 7 phase 4 cars reach 500kN were five of 7 MPV's reach this value .

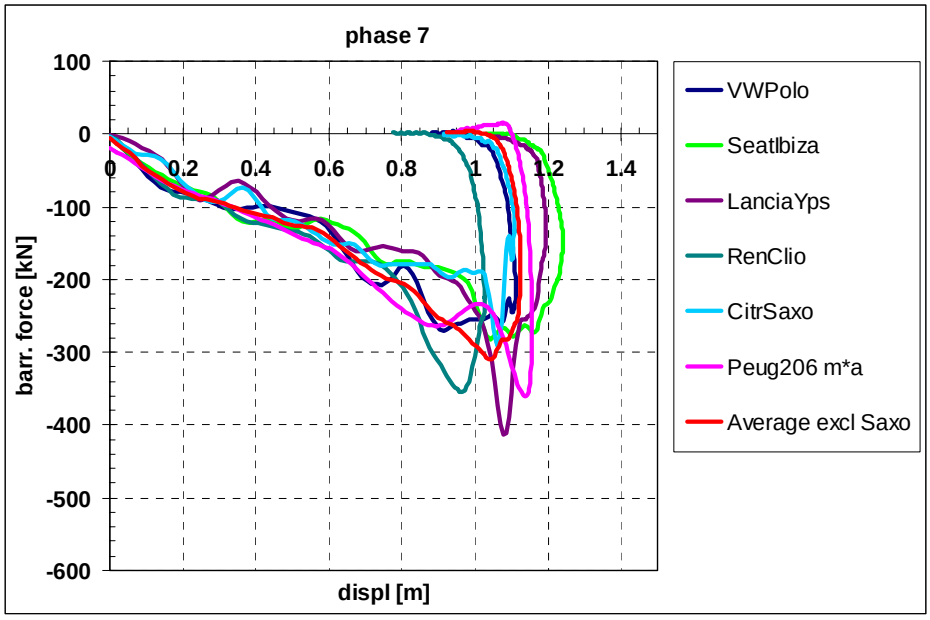

Figure 21 Overview phase 7 small family cars.

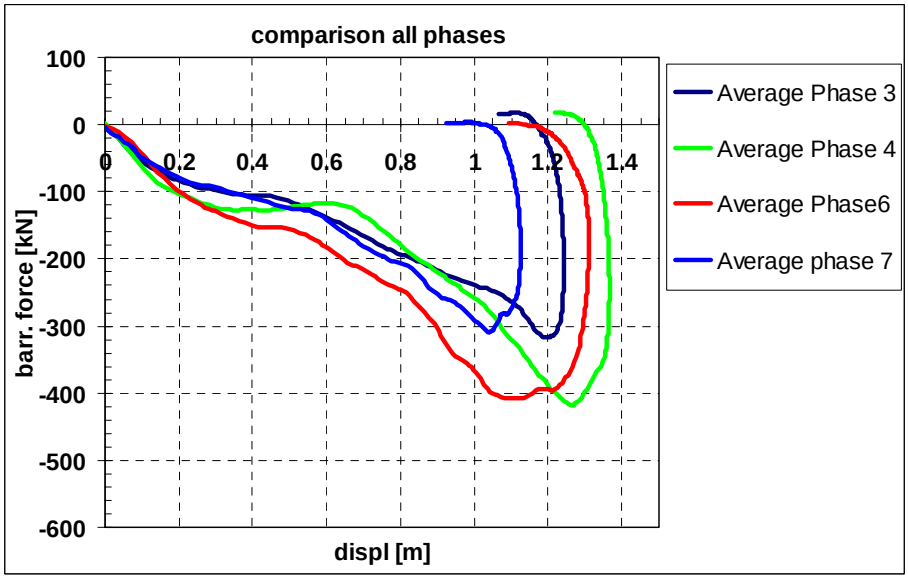

Figure 22 Comparison averages all car categories.

CONCLUSIONS

General

1. The load distribution shows a dominant influence of the engine contact.
2. Trends for force displacements derived from acceleration times mass are basically the same as those derived from loadcell data with some exceptions.
3. The barrier seems to give an average resistance of about 100 kN until bottoming out at about 400 mm.
4. Phase 3 (medium size family cars) and 4 (large executive cars) show about the same force displacement curves up to 1200 mm where phase 3 cars stop and phase 4 cars build up a higher load to account for the extra energy absorption because of the higher masses.
5. Phase 7 (small family cars) show the same force displacement curves as 3+4 up to 800 mm. After that a progressive increase can be observed up to the maximum displacement of 1100 mm.
6. Phase 6 (MPV's) show the same characteristic up to 600 mm after which a rapid increase of the load can be observed.

With regard to Compatibility

1. ENCAP loadcell data cannot be used to assess the homogeneity of a vehicle front. The engine area shows an overwhelming influence on the total load distribution pattern. The structural influence cannot be distinguished. The barrier face filters out this influence. Other test methods have to be developed for this assessment.
2. ENCAP loadcell data gives a good impression on the global stiffness of the current vehicle types. It is recommended to use loadcell barriers for each ENCAP test to monitor the global stiffnesses of cars.
3. Because of the large contribution of the engine area to the total load, this area gives a high potential to provide a good interaction between cars, as long as these area's overlap in a frontal car-car crash. For side impact this is not beneficial.
4. Looking to the global stiffnesses only, phase 3,4 and 7 look quite "compatible". Each type of car is able to deform any other type of car. Even the small family car can deform the large executive car. This does not mean that for each collision speed this compatibility statement is true. For a collision of a small car against a heavy vehicle, the vehicles are compatible to a speed where the maximum energy is absorbed for the lighter vehicle. Above that speed the small vehicle might collapse or might take more energy. A test with a higher speed (overload test) would be necessary to give that answer.
5. Phase 6 vehicles, because of their higher mass and stiffness can be considered as more aggressive to the others and will overload the other cars at a lower collision speed. This negative trend can only be changed by increase of the crushable space of the MPV's.
6. The trend of increased vehicle front stiffness should be reflected in the barrier characteristic for the European side impact regulation, since the current characteristic is based on the average of old cars.

ACKNOWLEDGMENTS.

The authors gratefully acknowledge the EuroNcap Programme Partnership who made the data used in this paper available. Readers are encouraged to visit the EuroNcap web-site www.euroncap.com.

The authors thank TRL and TNO in their cooperation in the data processing, needed to carry out this analyses, which hopefully leads to a better understanding in what directions future vehicle designs have to go for improved compatibility and improved overall passive safety.

REFERENCES

1 Richter, B., e.a., *Entwicklung von PKW im Hinblick auf einen volkswirtschaftlich optimalen Insassenschutz*, ROSI-Rapport (in German), Germany, 1984.

2 Hollowell, W.T., and Gabler, H.C., 'NHTSA's Vehicle Aggressivity and Compatibility Research program', 15th Int. *Technical Conf. on the Enhanced Safety of Vehicles*, Melbourne, Australia, May 13-17, 1996.

3 Evans, L., and Frick, M.C., 'Driver fatality risk in two-car crashes -- dependence on masses of driven and striking cars', in Proc. of the *13th ESV Conf.*, paper no. 91-S1-O-10, Paris, France, 1991.

4 Hollowell, W.T., and Gabler, H.C., 'NHTSA's Vehicle Aggressivity and Compatibility Research program', 15th Int. *Technical Conf. on the Enhanced Safety of Vehicles*, Melbourne, Australia, May 13-17, 1996.

5 Zeidler, F., Knöchelmann, F., 'The influence of Frontal Crash Test Speeds on the compatibility of Passenger Cars in Real World Accidents', in: VDI Tagungsbericht 1354, *Innovativer Insassenschutz im PKW*, pp. 37-52, Düsseldorf, Germany, 1997.

6 Faerber, E., 'Improvement of crash compatibility between cars', (project summary), *Conference on road infrastructure and safety research in Europe, Risc '97*, Brussels, 1997.

7 Hobbs, C.A., Williams, D.A., and Coleman, D.J., 'Compatibility of cars in frontal and side impact', 15th Int. *Techn. Conf. on Enhanced Safety of Vehicles* (paper no. 96 S4 O 05), Melbourne, Australia, 1996.

8 Shearlaw, A., and Thomas, P., ' Vehicle to vehicle compatibility in real world accidents', Proc. of the *15th ESV conference*, paper no. 96-S4-O-04, 1996.

9 Zobel, R., 1997, 'Barrier impact tests and demands for compatibility of passenger vehicles', in: VDI Tagungsbericht 1354, *Innovativer Insassenschutz im PKW*, pp. 209-225, Düsseldorf, Germany, 1997.

10 MPV Crash Test Results EuroNcap June 1999